Collective oscillations, bicluster motion, and dynamical order in a system of globally coupled rotors with repulsive interactions

Daun Jeong,[1] J. Choi,[2] and M. Y. Choi[1,3]
[1]*Department of Physics and Center for Theoretical Physics, Seoul National University, Seoul 151-747, Korea*
[2]*Department of Physics, Keimyung University, Daegu 704-701, Korea*
[3]*Korea Institute for Advanced Study, Seoul 130-722, Korea*
(Received 13 June 2005; revised manuscript received 2 July 2006; published 7 November 2006)

We perform extensive numerical simulations on a system of globally coupled rotors with repulsive interactions. By controlling systematically initial conditions, we determine the criterion for the emergence of bicluster motion. It is found that stable bicluster motion emerges at low temperatures, where the initial kinetic energy accounts for less than about 60% of the total energy. Also observed are collective oscillations of the potential energy and the magnetization, which are persistent. With appropriately chosen initial conditions, the system exhibits characteristic motion where biclusters keep forming and disappearing continually. It is argued that such bicluster motion is closely related to the dynamical order suggested recently.

DOI: 10.1103/PhysRevE.74.056106 PACS number(s): 05.20.−y, 05.45.−a

During the past decade the system of globally coupled classical rotors with sinusoidal interactions, which simulates physical systems with long-range interactions [1], has been the subject of extensive studies [2]. Here the interaction range is infinite with the strength scaling with the system size, making the system of mean-field character and thus amenable analytical treatment. Specifically, in the canonical ensemble, describing thermal equilibrium, the system with attractive interactions undergoes an equilibrium phase transition at a finite critical temperature, below which rotors move coherently as a single group (monocluster). On the other hand, there is no phase transition for repulsive interactions, implying that rotors move incoherently at all temperatures.

These predictions are confirmed in direct dynamical simulations (based on the microcanonical ensemble), which further disclose rich dynamical behaviors present in the system [3–9]. For example, the attractive system displays extremely slow relaxation toward thermodynamic equilibrium. This slow relaxation, dubbed quasistationarity, does not coincide with the predictions in the canonical ensemble, and thus the suggestion has been made that there may exist inequivalence between canonical and microcanonical ensembles. Such quasistationarity is observed to survive well below the equilibrium critical temperature. It has also been reported that the system exhibits many other interesting behaviors in the regime of quasistationarity [5,8,10].

For repulsive interactions, the system exhibits different coherent motion persisting for a long time: The rotors move in two groups, forming a bicluster, for some initial conditions in dynamic simulations [11]. Such coherent motion with the bicluster formation emerges at low temperatures or energies, and goes away as the temperature is raised. This has led to the surmise that the bicluster corresponds to an equilibrium of some effective dynamics [12]. Recent work, however, has argued that the bicluster formation results from other dynamic effect of the globally coupled system, i.e., dynamical order allowed by rotating solutions of the associated Fokker-Planck equation (FPE) [13], raising controversy as to the nature of this motion. In this work we perform extensive dynamic simulations with systematically controlled initial conditions and determine the criterion for the formation of biclusters. Revealed is the important role of the initial potential energy in the bicluster formation. Specifically, for given total energy, larger values of the potential energy facilitate the formation of biclusters, manifesting the importance of interactions between rotors. Furthermore, starting from a perfect bicluster state, the system exhibits characteristic motion where biclusters keep forming and disappearing continually; this bicluster motion, apparently different from the "stable" bicluster motion, may be attributed to the dynamical order allowed by rotating solutions of the FPE.

The dynamics of a system of N globally coupled rotors with repulsive interactions is governed by the set of equations of motion for the phase ϕ_i of the ith rotor $(i=1,\ldots,N)$

$$I\ddot{\phi}_i - \frac{J}{N}\sum_j \sin(\phi_i - \phi_j) = 0 \tag{1}$$

where I and J denote the (rotational) inertia of each rotor and the coupling strength between rotors, respectively. Rescaling time t in units of $\sqrt{I/J}$, we write Eq. (1) in the dimensionless form

$$\ddot{\phi}_i - \frac{1}{N}\sum_j \sin(\phi_i - \phi_j) = 0. \tag{2}$$

With the introduction of the canonical momentum $p_i = \dot{\phi}_i$, Eq. (2) obtains the form of a set of canonical equations with the total energy

$$E = \sum_i \frac{p_i^2}{2} + \frac{1}{N}\sum_{i<j} \cos(\phi_i - \phi_j) \equiv K + V, \tag{3}$$

where the time evolution of the kinetic energy K and that of the potential energy V are to be closely monitored in simulations. Coherence in the system is measured by the generalized order parameter M_ℓ $(\ell=1,2,\ldots)$ defined according to

$$\frac{1}{N}\sum_{i}^{N} e^{i\ell\phi_i} \equiv M_\ell e^{i\theta_\ell}. \tag{4}$$

For instance, the order parameter with $\ell=1$ measures the monocluster (magnetization) and that with $\ell=2$ the bicluster, respectively.

We begin with the initial conditions of phases $\{\phi_i\}$ and momenta $\{p_i\}$ used in our simulations. As for $\{\phi_i\}$, a uniform distribution is taken and the potential energy $V(t=0)\equiv V_0$ for this configuration is calculated. Due to random assignment of initial phases, the initial potential energy V_0 may not be controlled precisely. Instead, we divide the range of the total energy into ten segments and set V_0 in one of the ten segments. With the initial phases adopted to give the corresponding energy, the system may be partially clustered initially, i.e., having small values of $M_1(t=0)$. Starting from the initial phases prepared in this way, we observe the relaxation to the equilibrium state with a variety of momentum distributions. Next, we assign the frequently used "waterbag" distribution for $\{p_i\}$, to satisfy $K(t=0)\equiv K_0=E-V_0$ for given total energy E and vanishing total momentum. This nonequilibrium initial condition is controlled by means of the total energy density $U=E/N$ and the initial potential energy V_0. We employ the fourth-order symplectic scheme [14] to integrate the equations of motion for N rotors. In general, systems with the size (i.e., the number of rotors) N larger than 100 are observed to give no appreciable difference as far as the bicluster formation is concerned; we consider mostly the system of $N=800$ rotors, and measure various quantities including M_1, M_2, K, and V as functions of time t. With the time step $\Delta t=0.01$ taken in the integration, the typical errors are controlled within the range $O(10^{-9})$ to $O(10^{-11})$, depending on the kinetic energy. In particular, varying the energy density U from 10^{-5} to 10^{-2} (in units of J), we search for the conditions that lead to the bicluster structure, described by M_2. For given total energy E, we adopt the ratio $\gamma=V_0/E$ of the initial potential energy to the total energy as a control parameter, to find the dependence on the initial potential energy. It is observed that the bicluster order parameter M_2, increases gradually from the initial value $M_2(t=0)\approx 0$ and exhibits damped oscillatory motion. Its overall variations are much slower than those of the magnetization M_1, which also exhibits oscillations (see Fig. 1), and in addition there are small fast oscillations along the overall slow oscillatory behavior. After the transient behavior, the amplitude of slow oscillations reduces with increasing system size, similarly to a thermodynamic quantity in the canonical ensemble. In contrast, fast oscillations are observed to persist in the stationary state. These behaviors characterize the long-range (global) coupling of the system, which gives rise to plasma oscillations. The stationary values of measured quantities are thus obtained by taking time averages, typically through $t=10^6$, with the data from the first 5×10^5 time steps discarded; this appears to be sufficient for attaining stationarity.

At stationarity we define the temperature T as a measure of the average kinetic energy according to $T/2\equiv\langle p^2\rangle/2=K/N$, which may be different from the initial temperature $T_0=2K_0/N$. We find the (stationary) value of the bicluster

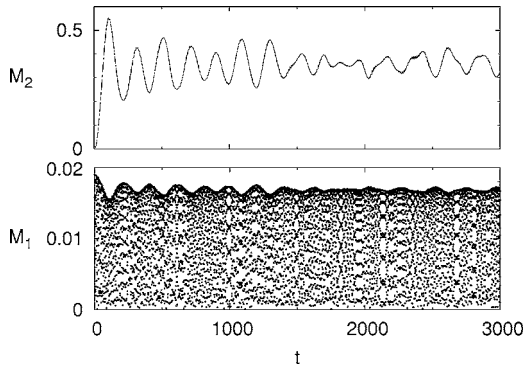

FIG. 1. Typical time evolution of the order parameters M_2 and M_1 of a system of $N=200$ rotors at $U=2\times 10^{-4}$ with $\gamma=0.75$. M_2 exhibits oscillatory motion consisting of fast smaller oscillations. M_1 also exhibits oscillations, in general smaller and faster than those of M_2.

order parameter M_2 to vanish at high temperatures ($T\gtrsim 5\times 10^{-3}$ in units of J with the Boltzmann constant $k_B\equiv 1$) for any initial configuration [15], which is consistent with Ref. [11]. However, as shown in Fig. 2(a), when the initial potential energy is less than about 60% of the total energy, we do not observe bicluster structure even at the lowest temperature considered. In terms of the parameter $T/U=2(1-\langle V\rangle/E)$, which measures the ratio of the kinetic energy to the total energy, the data are conveniently replotted in Fig. 2(b). It is clearly demonstrated that distinctive biclusters are formed only for small values of T/U, say, less than 1.3, implying that large momentum fluctuations tend to prohibit the formation of biclusters.

Heretofore we have considered only the uniform (waterbag) distribution of the initial momenta. Two momentum distributions other than the uniform distribution are also considered: One is the Maxwell distribution $f(p)\propto\exp(-p^2/2T_0)$ with the initial temperature $T_0\equiv 2(U-V_0/N)$, and the other is the sinusoidal distribution, where the initial momentum of each rotor depends on its initial phase according to $p_i=c\sin\phi_i$. Here c is related to the kinetic energy via $K/N=\langle p^2\rangle$, which reads $c^2=NT_0(\Sigma_i\sin^2\phi_i)^{-1}$. In the case of uniform distribution of the initial phases, we thus have $c=\sqrt{2T_0}$ with the initial temperature T_0. For the Maxwell distribution, the overall results, shown in Fig. 3(a), are qualitatively similar to those of the waterbag distribution. Biclusters are formed when $T/U\lesssim 1.3$, again manifesting the dependence on the initial potential energy. In the case of the sinusoidal distribution, on the other hand, one always observes biclusters regardless of the initial potential energy for given energy density, if the temperature is low enough ($T\lesssim 3\times 10^{-3}$) [see Fig. 3(b)]. This may be understood as follows. In the sinusoidal distribution of initial momenta, rotors with phases in the range $[0,\pi)$ have momenta opposite to those in the range $[\pi,2\pi)$ initially. This gives a drift to the rotors, assisting them to get together. As a result, the system can develop far larger M_1 than the initial value and the average potential energy grows, which is not observed in the case of other initial conditions. It is of interest that M_2 changes nonmonotonically and exhibits a peak as T/U is varied; the physical meaning of the peak needs more investigation.

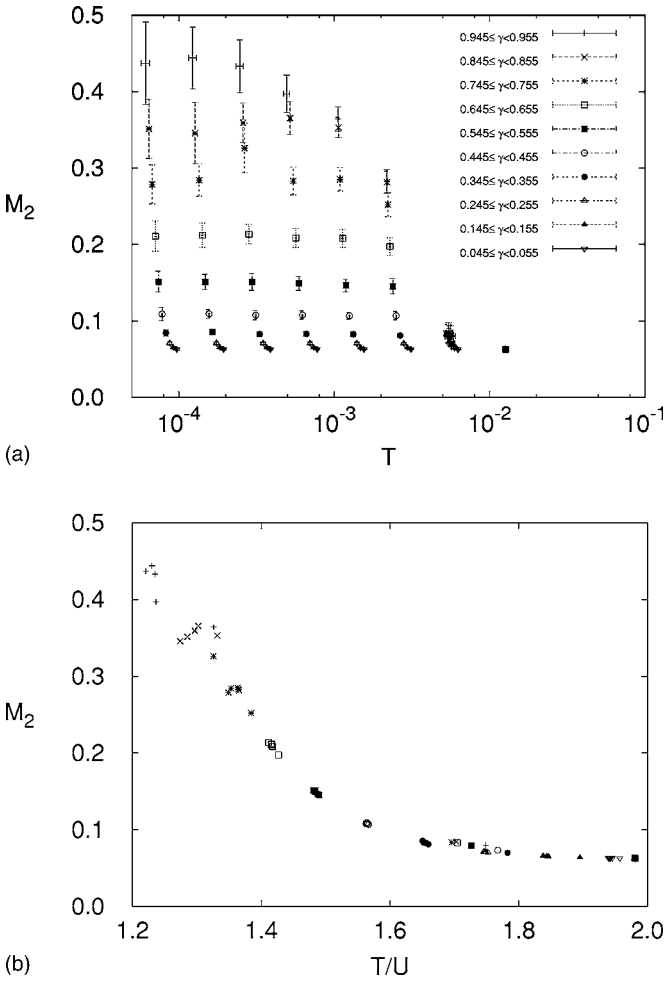

FIG. 2. (a) Bicluster order parameter M_2 versus temperature T (in units of J). Data have been taken from the average over time in the stationary state. Different symbols correspond to different values of the ratio of the initial potential energy to the total energy, $\gamma \equiv V_0/E$. (b) The same data are plotted versus the rescaled temperature (in units of the energy density U). Manifested is the localized structure, characterized by the bicluster formation, at low temperatures and/or large initial potential energies ($T/U \lesssim 1.3$).

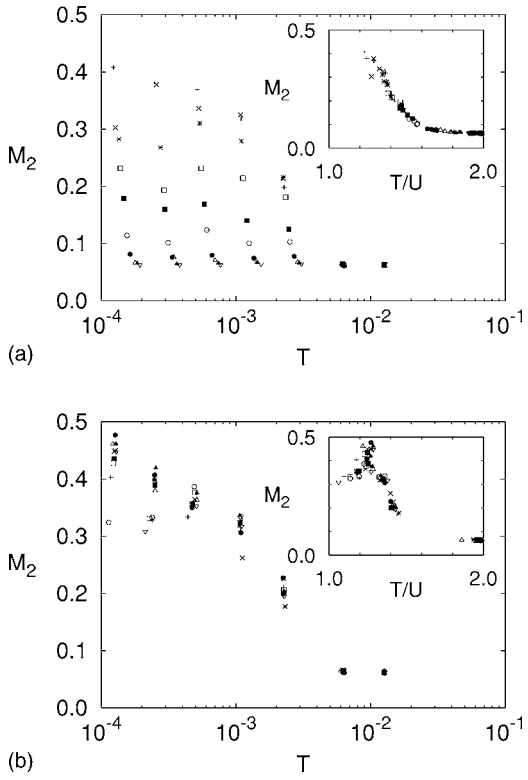

FIG. 3. Bicluster order parameter M_2 versus the temperature T for (a) the Maxwell distribution and (b) the sinusoidal distribution of initial momenta. Symbols represent the same as those in Fig. 2. Whereas results shown in (a) are qualitatively the same as those from the waterbag distribution, (b) demonstrates the formation of biclusters at low temperatures regardless of the initial potential energy. Insets display the same data for M_2 plotted versus T/U.

Another interesting phenomenon to be noted here is the rapid oscillations of the potential energy. As presented in Fig. 4, the potential energy V exhibits fast oscillations with very small amplitude, which varies slowly in time as well. Here it is tempting to consider the envelope of the fast oscillations, i.e., a slow variation of the amplitude, to be the effective potential experienced by the rotors; this stays parallel with the suggestion on the effective dynamics obtained by integrating out fast variables [12], in which the effective potential V_{eff} is expressed in terms of M_2. It is thus of interest to test the prediction of the effective dynamics theory as to the potential energy oscillations observed in our simulations. To this end, we compare the envelope of the potential energy oscillations with the effective potential, which depends on M_2 according to $V_{\text{eff}} \sim (1-M_2)^{1/2}$. In Fig. 4 we display typical effective potential fits for two different values of the initial potential energy V (but with the same energy density U). When the initial potential energy is large [see Fig. 4(a) where $T/U=1.28$], the envelope agrees very well with the effective potential form. Such excellent agreement persists at the long time as well. We point out that the initial conditions adopted in Ref. [11] indeed belong to this regime (i.e., $T/U \lesssim 1.3$). However, for general initial conditions with small relative variations of the potential energy, the potential energy oscillations gradually deviate from the above effective dynamics as T/U is raised beyond 1.3 [see Fig. 4(b) where $T/U=1.58$]. In this regime biclusters fade away. This indicates that the effective dynamics theory provides only a partial answer to the bicluster motion, not explaining the mechanism of its formation.

We now discuss the rapid oscillation of the potential energy V and its role in the bicluster formation. Since $V \propto M_1^2$, the time series of M_1 also exhibits a complex oscillatory behavior, the amplitude of which lies between $M_1(t=0)$ and zero. This type of oscillation, persisting for a very long time, has also been reported in a system of globally coupled rotors with attractive interactions and suggested to be the inherent behavior of the globally coupled system [10]. Naturally, both the kinetic energy and the potential energy also oscillate with amplitudes depending on the initial conditions. We presume that such collective oscillations are indicative of metastability. In Ref. [10] it has been suggested that the collective motion, interpreted as the self-organization of self-excited rotors in a globally coupled system, is a characteristic of the

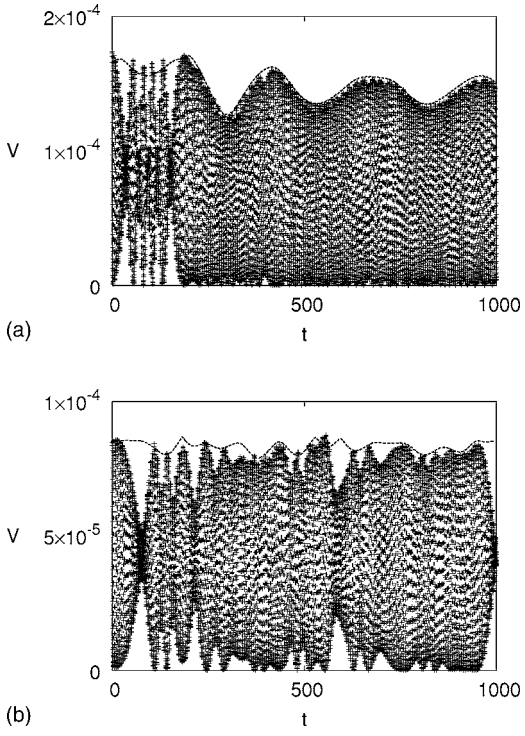

FIG. 4. Potential energy oscillations in comparison with the effective potential energy for two different initial potential energy ratios $\gamma=$ (a) 0.87 and (b) 0.42 with $U=2.0\times10^{-4}$. Dashed curves correspond to the effective potential energy $C\sqrt{1-M_2}$ with $C=$(a) 1.73×10^{-4} and (b) 8.7×10^{-5}. The case (a), corresponding to $T/U=1.28$, shows good agreement with the effective dynamics; such agreement is not observed in (b) where $T/U=1.58$.

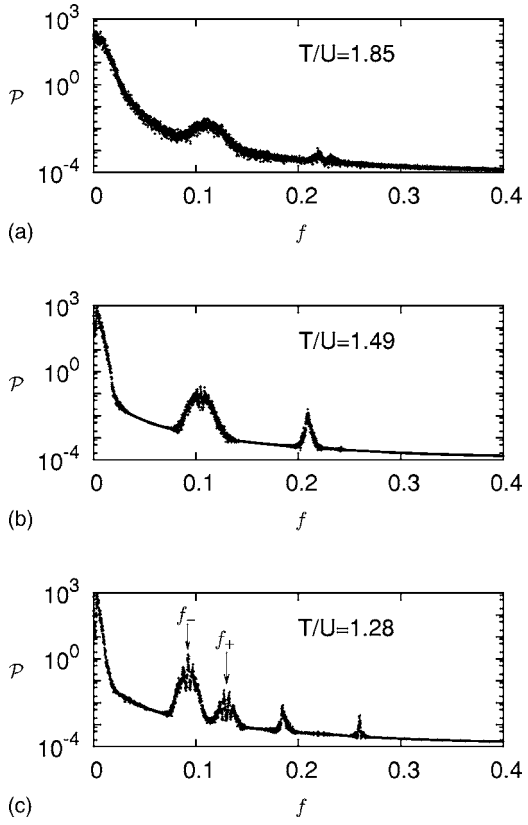

FIG. 5. Power spectrum of M_2, denoted by $\mathcal{P}$, versus the frequency f for various values of T/U. The two normal modes $f_\pm$ are indicated in (c).

mean-field system. It is thus of interest to examine the physical origin of these excited modes and the mechanism of their sustenance.

Note first that this oscillatory behavior emerges regardless of the energy density. To examine it, we compute the power spectrum of M_2 for various values of T/U and display some typical results in Fig. 5, where the main peaks together with higher harmonics are observed. In particular, as the temperature is lowered, the main peak in the power spectrum $\mathcal{P}$ is shown to develop, manifesting that biclusters formed with increasing amplitude. At sufficiently low temperatures where biclusters are formed (i.e., $T/U\lesssim1.3$), the amplitude of oscillations is found not to vary as a whole. It is also observed that the major peak splits into two peaks. This may be understood as follows. As described before, the initial potential energy V_0, a function of the initial phases $\{\phi_i^0\}$, affects the formation of the bicluster. We therefore consider small perturbations around the initial phases and write

$$\phi_i = \phi_i^0 + \epsilon_i. \tag{5}$$

Substitution of this into Eq. (2) and linearization lead to

$$\ddot{\epsilon}_i + \frac{1}{N}\sum_{j=1}^{N} \epsilon_j \cos(\phi_i^0 - \phi_j^0) = 0, \tag{6}$$

the solution of which may be obtained from diagonalizing the matrix

$$V_{ij} = \frac{1}{N}\cos(\phi_i^0 - \phi_j^0). \tag{7}$$

The nonzero eigenvalues or the normal mode frequencies are given by [12]

$$\omega_\pm^2 = \frac{1 \pm |M_2|}{2}, \tag{8}$$

which reveals that the single normal mode $\omega\equiv2\pi f=1/\sqrt{2}$ present for $M_2=0$ indeed splits into two modes $\omega_\pm=2\pi f_\pm$ as the bicluster develops [see Fig. 5(c)]. Therefore relatively large values of the initial potential energy V_0 initiate the formation of the bicluster, which in turn contributes the normal modes in M_2 and induces splitting. For a simple uniform distribution, it is straightforward to show, via direct calculation of the eigenvalues of $V_{ij}=N^{-1}\cos[2\pi N^{-1}(i-j)]$, that there is only one normal mode $\omega=1/\sqrt{2}$. This implies that from the uniform distribution it is hard to develop the bicluster perturbatively, which is also consistent with the observation that the bicluster is easily formed for large potential energies.

In addition, initial conditions with nonzero M_2 may facilitate the bicluster formation. To illustrate this, we set the system perfectly biclustered initially, i.e., $\phi_i(0)=0$ for $i=1,\ldots,N/2$ and $\phi_i(0)=\pi$ for $i=N/2+1,\ldots,N$ and measure the bicluster order parameter M_2, the evolution of which is plotted in Fig. 6. It is observed that M_2 varies continuously

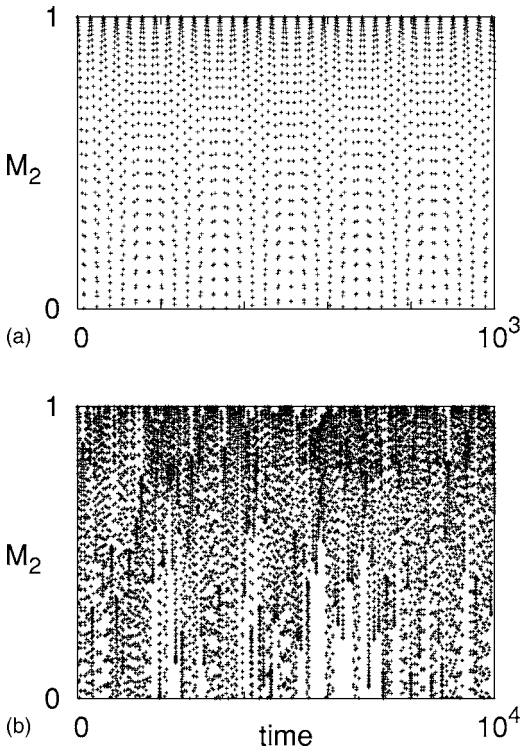

FIG. 6. Bicluster order parameter M_2 versus time t for two different initial momentum distributions: (a) $\dot{\phi}_i(0)=\dot{\phi}_{N-i}(0)=v$ for $i=1,\ldots,N/4$ and $-v$ for $i=N/4+1,\ldots,N/2$; (b) $\dot{\phi}_i(0)=-\dot{\phi}_{N-i}(0)=v_1$ for $i=1,\ldots,N/4$ and v_2 for $i=N/4+1,\ldots,N/2$.

from 0 to 1. In Fig. 6(a), each rotor in a cluster has its counterpart in another which has the same momentum, and biclusters are observed to form and disappear continuously. Here the net force exerted on a particular rotor always vanishes since the force produced by a rotor within the same cluster is canceled by that in the other cluster. Each rotor thus keeps its own initial momentum and its phase grows linearly in time, yielding the oscillatory behavior of M_2. In Fig. 6(b), on the other hand, four values of the initial momentum just make the total momentum vanish and four clusters interact with each other, still leading to (more complex) oscillations of M_2 between 0 and 1. We remark that the oscillations in Figs. 6(a) and 6(b) persist indefinitely and only parts of them are displayed. Here rotors in each cluster move as a single particle, which makes the system equivalent to a system of four rotors displaying large fluctuations of M_2 (between 0 and 1). The range of M_2 in general reduces with the number of clusters.

Apparently these bicluster motions are different from those in Ref. [11]. In the latter each rotor exhibits a small oscillatory motion around the long-time trajectory which should vanish if "fast variables" are integrated out as claimed in Ref. [12]. It is, however, obvious that there are no fast variables to be integrated out in Fig. 6(a). Meanwhile fast oscillations are observed in Fig. 6(b), but the behavior of M_2 varies greatly, depending sensitively on the initial conditions. Further, these results do not depend on specific values of initial velocities, which implies that bicluster motion of this type is independent of the temperature.

Such bicluster motions observed in dynamic simulations are closely related with dynamical order present in the system, which may be demonstrated as follows. Using Eq. (4) with $\ell=1$ in Eq. (2), we get the single-particle equation from which one may derive the corresponding FPE for the single-rotor probability distribution $P(\phi,p,t)$ [13]. In the absence of thermodynamic order (i.e., $M_1=0$), the FPE reads

$$\frac{\partial P}{\partial t}=-p\frac{\partial P}{\partial \phi}. \tag{9}$$

It has been shown that $P(\phi,p,t)$ admits a rotating solution of the form [13]

$$P(\phi,p,t)=\sum_{k\neq\pm 1}\exp[ik(\phi-pt)]F_k(p), \tag{10}$$

which allows dynamical order with any degree of clustering other than the monocluster ($M_1=0$). For instance, as for the biclustering, it has been shown, with the choice $F_{2k}(p)=F(p)$ and $F_{2k+1}(p)=0$, that [13]

$$P(\phi,p,t)=\pi F(p)[\delta(\phi-pt)+\delta(\phi-pt+\pi)]. \tag{11}$$

It is then straightforward to show, for this distribution with $F(p)=(1/2)[\delta(p-v)+\delta(p+v)]$, that M_2 oscillates with frequency $2v$, which is observed in Fig. 6(a). It has further been shown that the rotating solution is neutrally stable at all temperatures for repulsive interactions, supporting the observation that the oscillatory behavior does not depend on the initial velocity v. For the perfect bicluster state ($M_2=1$), it is obvious that we have a single mode of $\omega=1$ and this mode persists as described before.

When there is velocity (momentum) dispersion such as v_1 and v_2 in Fig. 6(b), similar arguments lead to M_2 oscillations consisting of two frequencies $2v_1$ and $2v_2$, although the detailed behavior may vary, depending on the specific values of v_1 and v_2. For example, a slow frequency may also develop if the velocity difference is small. As more dispersion is introduced in the velocity distribution, it would be easier to develop slow collective oscillations in the midst of fast oscillations unless the width of the distribution is too wide.

This suggest that collective oscillations and bicluster motions are closely related. This is to be contrasted with the system with attractive interactions, which has self-excited modes via the Hopf bifurcation in the high-energy region [10].

To summarize, we have investigated the formation of a biclustered structure in a system of globally coupled rotors with repulsive interactions, using various initial conditions. It is revealed that the ratio of the initial potential energy to the total energy plays a crucial role in the spontaneous formation of biclusters. In particular, biclusters are formed only when the initial potential energy exceeds 60% of the total energy or $T/U\lesssim 1.3$. Also observed are collective oscillations in the system and a major peak shift to lower frequencies as biclusters are formed, indicating the role of collective oscillations in the formation of biclusters. Further, it has been

demonstrated that interesting bicluster motion can arise from dynamic effects, in which M_2 continuously varies between 0 and 1. This suggests that the bicluster formation is closely related to dynamical order [13]. With appropriate velocity (momentum) dispersion, this bicluster motion in turn develops slow collective oscillations and may become stabilized. The stabilized bicluster motion then could be well described by the effective dynamics [12].

This work was supported by a grant from the MOST/KOSEF to the NCRC for Systems Bio-Dynamics (Grant No. R15-2004-033) and by the BK21 Program.

[1] M. Antoni and S. Ruffo, Phys. Rev. E **52**, 2361 (1995).
[2] For a collection of review articles, see *Dynamics and Thermodynamics in Systems with Long-Range Interactions*, edited by T. Dauxois, S. Ruffo, E. Arimondo, and M. Wilkens, Lecture Notes in Physics Vol. 602 (Springer, Berlin, 2002).
[3] V. Latora, A. Rapisarda, and S. Ruffo, Phys. Rev. Lett. **80**, 692 (1998); **83**, 2104 (1999); Physica A **280**, 81 (2000).
[4] V. Latora, A. Rapisarda, and C. Tsallis, Phys. Rev. E **64**, 056134 (2001); Physica A **305**, 129 (2002).
[5] M. A. Montemurro, F. Tamarit, and C. Anteneodo, Phys. Rev. E **67**, 031106 (2003).
[6] Y. Y. Yamaguchi, Phys. Rev. E **68**, 066210 (2003).
[7] D. H. Zanette and M. A. Montemurro, Phys. Rev. E **67**, 031105 (2003).
[8] A. Pluchino, V. Latora, and A. Rapisarda, Physica D **193**, 315 (2004).
[9] Y. Y. Yamaguchi, J. Barré, F. Bouchet, T. Dauxois, and S. Ruffo, Physica A **377**, 36 (2004).
[10] H. Morita and K. Kaneko, Phys. Rev. Lett. **96**, 050602 (2006).
[11] T. Dauxois, P. Holdsworth, and S. Ruffo, Eur. Phys. J. B **16**, 659 (2000).
[12] J. Barré, F. Bouchet, T. Dauxois, and S. Ruffo, Eur. Phys. J. B **29**, 577 (2002); J. Barré, F. Bouchet, T. Dauxois, and S. Ruffo, Phys. Rev. Lett. **89**, 110601 (2002).
[13] M. Y. Choi and J. Choi, Phys. Rev. Lett. **91**, 124101 (2003); J. Choi and M. Y. Choi, J. Phys. A **38**, 5659 (2005).
[14] H. Yoshida, Phys. Lett. A **150**, 262 (1990).
[15] Note here that the apparent nonzero value of M_2 reflects finite-size effects; we have confirmed that it vanishes as $N^{-1/2}$ with the system size N.